

Polymer-stabilized blue-phase liquid crystal grating cured with interfered visible light

Yachao Yuan, Yan Li,* Chao Ping Chen, Shuxin Liu, Na Rong, Weihuan Li, Xiao Li, Pengcheng Zhou, Jiangang Lu, Ruili Liu, and Yikai Su

National Engineering Lab for TFT-LCD Materials and Technologies, Department of Electronic Engineering, Shanghai Jiao Tong University, Shanghai 200240, China
yan.li@sjtu.edu.cn

Abstract: In this paper, we demonstrate a holographic polymer-stabilized blue-phase liquid crystal grating fabricated using a visible laser. As blue phase is stabilized by the interfered light, polymer-concentration gradient is achieved simultaneously. With the application of a uniform vertical electric field, periodic index distribution is obtained due to polymer-concentration gradient. The grating exhibits several attractive features such as polarization-independency, a broad temperature range, sub-millisecond response, simple fabrication, and low cost, thus holding great potential for photonics applications.

©2015 Optical Society of America

OCIS codes: (230.3720) Liquid-crystal devices; (050.2770) Gratings; (090.2890) Holographic optical elements.

References and links

1. T. O. Carroll, "Liquid-crystal diffraction gratings," *J. Appl. Phys.* **43**(3), 767–770 (1972).
2. L. Gu, X. Chen, W. Jiang, B. Howley, and R. T. Chen, "Fringing-field minimization in liquid-crystal-based high-resolution switchable gratings," *Appl. Phys. Lett.* **87**(20), 201106 (2005).
3. C. M. Titus and P. J. Bos, "Efficient, polarization-independent, reflective liquid crystal phase grating," *Appl. Phys. Lett.* **71**(16), 2239–2241 (1997).
4. J. Chen, P. J. Bos, H. Vithana, and D. L. Johnson, "An electro-optically controlled liquid-crystal diffraction grating," *Appl. Phys. Lett.* **67**(18), 2588–2590 (1995).
5. R. L. Sutherland, V. P. Tondiglia, L. V. Natarajan, T. J. Bunning, and W. W. Adams, "Electrically switchable volume gratings in polymer-dispersed liquid crystals," *Appl. Phys. Lett.* **64**(9), 1074–1076 (1994).
6. D. P. Resler, D. S. Hobbs, R. C. Sharp, L. J. Friedman, and T. A. Dorschner, "High-efficiency liquid-crystal optical phased-array beam steering," *Opt. Lett.* **21**(9), 689–691 (1996).
7. R. K. Komanduri, W. M. Jones, C. Oh, and M. J. Escuti, "Polarization-independent modulation for projection displays using small-period LC polarization gratings," *J. Soc. Inf. Disp.* **15**(8), 589–594 (2007).
8. D. Xu, G. Tan, and S. T. Wu, "Large-angle and high-efficiency tunable phase grating using fringe field switching liquid crystal," *Opt. Express* **23**(9), 12274–12285 (2015).
9. J. Sun and S. T. Wu, "Recent advances in polymer network liquid crystal spatial light modulators," *J. Polym. Sci. Pol. Phys.* **52**(3), 183–192 (2014).
10. J. Sun, S. Xu, H. Ren, and S. T. Wu, "Reconfigurable fabrication of scattering-free polymer network liquid crystal prism/grating/lens," *Appl. Phys. Lett.* **102**(16), 161106 (2013).
11. H. Kikuchi, M. Yokota, Y. Hisakado, H. Yang, and T. Kajiyama, "Polymer-stabilized liquid crystal blue phases," *Nat. Mater.* **1**(1), 64–68 (2002).
12. F. Castles, F. V. Day, S. M. Morris, D. H. Ko, D. J. Gardiner, M. M. Qasim, S. Nosheen, P. J. W. Hands, S. S. Choi, R. H. Friend, and H. J. Coles, "Blue-phase templated fabrication of three-dimensional nanostructures for photonic applications," *Nat. Mater.* **11**(7), 599–603 (2012).
13. L. Rao, Z. Ge, S. T. Wu, and S. H. Lee, "Low voltage blue-phase liquid crystal displays," *Appl. Phys. Lett.* **95**(23), 231101 (2009).
14. H. J. Coles and M. N. Pivnenko, "Liquid crystal 'blue phases' with a wide temperature range," *Nature* **436**(7053), 997–1000 (2005).
15. Z. Ge, S. Gauza, M. Jiao, H. Xianyu, and S. T. Wu, "Electro-optics of polymer-stabilized blue phase liquid crystal displays," *Appl. Phys. Lett.* **94**(10), 101104 (2009).
16. J. Yan, Y. Li, and S. T. Wu, "High-efficiency and fast-response tunable phase grating using a blue phase liquid crystal," *Opt. Lett.* **36**(8), 1404–1406 (2011).
17. J. Zhu, J. G. Lu, J. Qiang, E. Zhong, Z. Ye, Z. He, X. Guo, C. Dong, Y. Su, and H. P. D. Shieh, "1D/2D switchable grating based on field-induced polymer stabilized blue phase liquid crystal," *J. Appl. Phys.* **111**(3), 033101 (2012).

18. L. Yang, J. Xia, X. Zhang, Y. Xie, M. Kang, and Q. Zhang, "Fringing field suppression for liquid crystal gratings using equivalent capacitance configuration," *Jpn. J. Appl. Phys.* **53**(10), 102201 (2014).
19. Y. Lin, H. C. Jau, and T. H. Lin, "Polarization-independent rapidly responding phase grating based on hybrid blue phase liquid crystal," *J. Appl. Phys.* **113**(6), 063103 (2013).
20. J. Yan, Q. Li, and K. Hu, "Polarization independent blue phase liquid crystal gratings based on periodic polymer slices structure," *J. Appl. Phys.* **114**(15), 153104 (2013).
21. Z. H. He, C. P. Chen, J. L. Zhu, Y. C. Yuan, Y. Li, W. Hu, X. Li, H. J. Li, J. G. Lu, and Y. K. Su, "Electrically tunable holographic polymer templated blue phase liquid crystal grating," *Chin. Phys. B* **24**(6), 064203 (2015).
22. Y. J. Liu and X. W. Sun, "Holographic polymer-dispersed liquid crystals materials, formation, and applications," *Adv. Optoelectron.* **2008**, 684349 (2008).
23. J. Yan, H. C. Cheng, S. Gauza, Y. Li, M. Jiao, L. Rao, and S. T. Wu, "Extended Kerr effect of polymer-stabilized blue-phase liquid crystals," *Appl. Phys. Lett.* **96**(7), 071105 (2010).
24. J. Tan, Y. Song, J. L. Zhu, S. B. Ni, Y. J. Wang, X. Y. Sun, J. G. Lu, B. R. Yang, and H. P. D. Shieh, "Blue phase LC/polymer Fresnel lens fabricated by holographics," *J. Disp. Technol.* **10**(2), 157–161 (2014).
25. J. Yan, M. Jiao, L. Rao, and S. T. Wu, "Direct measurement of electric-field-induced birefringence in a polymer-stabilized blue-phase liquid crystal composite," *Opt. Express* **18**(11), 11450–11455 (2010).
26. G. Zhao and P. Mouroulis, "Diffusion model of hologram formation in dry photopolymer materials," *J. Mod. Opt.* **41**(10), 1929–1939 (1994).
27. Y. Chen, D. Xu, S. T. Wu, S. Yamamoto, and Y. Haseba, "A low voltage and submillisecond-response polymer-stabilized blue phase liquid crystal," *Appl. Phys. Lett.* **102**(14), 141116 (2013).

1. Introduction

Liquid crystal (LC) based electrically tunable diffraction gratings are widely used in three-dimensional (3-D) displays, optical communications, beam steering and remote sensing, for their light weight, low cost, and low power consumption [1–7]. They are conveniently controlled by exploiting the electro-optical properties of liquid crystals [1–4]. However, with conventional nematic LCs, the responses of the gratings are relatively slow (~10–100 ms) [8]. Several approaches have been proposed to shorten the response time [8–10]. Xu *et al.* proposed a fringe field switching phase grating which improved the response time to ~3 ms at room temperature [8]; Sun *et al.* demonstrated a polymer network LC grating with sub-millisecond response and negligible scattering [10]. Nevertheless, most LC gratings are operated with strong dependency on the polarization state of the incident light, which causes half of the power loss if unpolarized incident light is used.

Recently, polymer-stabilized blue-phase liquid crystal (PSBPLC) is considered as a promising candidate for next-generation display and photonics applications for its sub-millisecond response time, no need for surface alignment, and an optically isotropic dark state [11–17]. Yan *et al.* developed the first PSBPLC based tunable phase grating using an in-plane switching (IPS) cell [16]. However, the grating is polarization dependent, and the use of patterned electrodes leads to limited spatial-frequency due to fringing field effect [18]. Some electrode-pattern-free PSBPLC based polarization-independent gratings using photo masks have been proposed, but the grating periods are large and the fabrication processes are complicated [19, 20]. He *et al.* developed an electrode-pattern-free polarization-independent BPLC grating by using a holographic polymer template [21]. However, without polymer stabilization, the blue phase temperature range of the holographic polymer template device is still very narrow, and the multi-step fabrication method involving washing out and refilling liquid crystals is rather complicated.

In this work, we propose a novel one-step holographic fabrication of a tunable phase grating based on PSBPLC. Instead of using conventional non-coherent ultraviolet (UV) light, we use a visible laser with high coherence as the curing light source. Being exposed to the interference light pattern, the blue phase structure is stabilized, and periodic polymer concentration variation is achieved simultaneously. With the application of a uniform vertical electric field, periodic birefringence is induced. Thus, the index contrast is obtained and light is diffracted. The holographic polymer-stabilized blue-phase liquid crystal (H-PSBPLC) grating exhibits several attractive features such as polarization-independency, a broad temperature range and sub-millisecond response. Furthermore, without patterned electrodes or photo masks, the simple holographic fabrication could achieve high spatial resolution at low cost.

2. Grating fabrication and working principle

Fig. 1 depicts the formation process of the H-PSBPLC grating. As shown in Fig. 1(a), a cell is assembled with two glass substrates, and filled with uniform BPLC precursor. The glass substrates are coated with a thin transparent indium-tin-oxide (ITO) film on the inner surfaces. The cell is exposed to the alternating dark and bright interference pattern. In the bright regions, polymerization preferentially occurs and more monomers are consumed. Thus a monomer concentration gradient between bright and dark regions is created, causing monomers to diffuse from the dark regions to adjacent bright regions [22], as shown in Fig. 1(b). Therefore, the concentration of polymer chains in the bright regions is larger than that in the dark regions, as shown in Fig. 1(c).

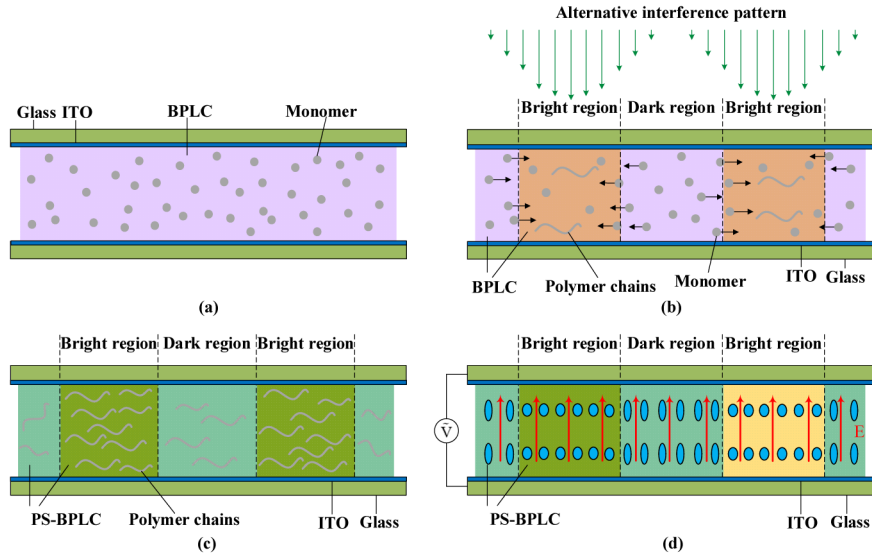


Fig. 1. Schematic diagram of the H-PSBPLC grating formation process: (a) uniform BPLC precursor filled into a cell; (b) cell exposure under holographic interference pattern and monomers diffusion from the dark regions to the bright regions; (c) periodic distribution of polymer chains after exposure; and (d) periodic birefringence distribution under a uniform vertical electric field.

At the voltage-off state, the PSBPLC is optically isotropic with an index n_{iso} . When an electric field is applied, the induced birefringence in a BPLC $\Delta n(E)$ can be described by the extended Kerr effect [23]

$$\Delta n(E) = \Delta n_{sat} \left[1 - \exp \left[- \left(\frac{E}{E_s} \right)^2 \right] \right], \quad (1)$$

where Δn_{sat} represents the saturated induced birefringence and E_s is the saturation field. The induced ordinary index $n_o(E)$ and extraordinary refractive index $n_e(E)$ can be expressed as below:

$$n_o(E) = n_{iso} - \Delta n(E) / 3, n_e(E) = n_{iso} + 2\Delta n(E) / 3. \quad (2)$$

In the bright regions, a larger volume fraction of the polymer chains leads to more rigid polymer network, and thus smaller birefringence is induced. On the contrary, in the dark regions, the polymer network is weaker, and induced birefringence larger with the same electric field. As a result, the periodic birefringence distribution is realized under a uniform vertical electric field as shown in Fig. 1(d). For normal incident light, both p and s waves

experience the same index $n_o(E)$, therefore, the grating operates independently of the polarization state.

3. Experiments and results

In our experiment, the BPLC precursor consisted of 85.4 wt% nematic liquid crystal host HTG135200-100 ($\Delta\epsilon = 57.2$ at 1 kHz and $\Delta n = 0.204@589\text{nm}$, HCCH), 4.0 wt% chiral dopant R5011 (HCCH), 4.0 wt% monomer TMPTA (Aldrich), 6.0 wt% monomer RM257 (HCCH), 0.3 wt% photoinitiator Rose Bengal (Aldrich), and 0.3% cointiator N-phenylglycine (Aldrich). They were mixed uniformly in the dark. The precursor was filled into the cell with a 20- μm cell gap via capillary action at 70 °C, and then cooled down to 62 °C at a rate of 0.1 °C/min. The BP temperature range of precursor is about 65 ~58 °C. Fig. 2(a) illustrates the experimental setup of the H-PSBPLC grating. Two beams generated by a Nd:YAG laser (532 nm, 100 mW, Coherent) intersected inside the cell and produced alternating bright and dark interference fringes. Each beam was set to *p*-polarization, with a power of 20 mW. The intersection angle was 7.6°. The holographic exposure time of the cell was 20 minutes, and after that the cell was exposed to UV light for 5 minutes to consume the residual monomers.

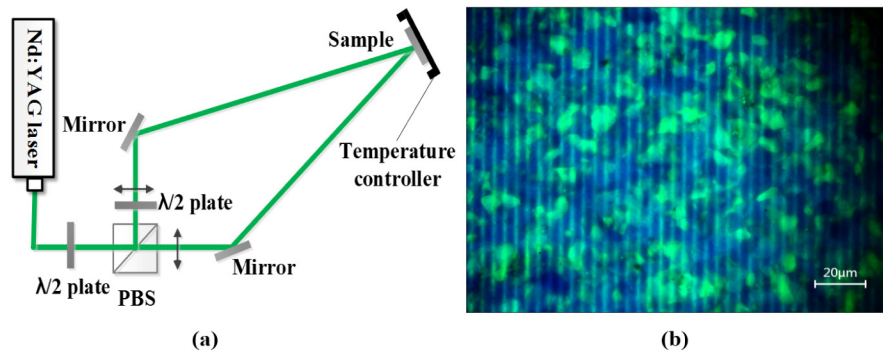


Fig. 2. (a) Experimental setup of fabricating the H-PSBPLC grating. PBS is a polarization beam splitter. (b) Platelet texture observed under an optical polarizing microscope of the H-PSBPLC grating at room temperature.

The morphologies of the H-PSBPLC grating are illustrated in Fig. 2(b), where the self-assembled BPLC exhibits a characteristic platelet texture when observed under an optical polarizing microscope in the reflective mode at room temperature. During the holographic exposure process, the polymer chains are selectively concentrated in the disclination lines in the cubic lattice of BP. Hence the double-twist cylinder construction of blue phase is stabilized and the temperature range of BP is broadened [11]. The temperature range of the H-PSBPLC grating is over 70 °C. Compared with the holographic polymer template BPLC devices [21, 24], the blue phase range is broadened and the one-step holographic fabrication method is much simpler. It can be seen that the grating period is about 4 μm , which is much smaller than conventional PSBPLC gratings using patterned electrodes [16, 17] or photo masks [19, 20]. During the holographic fabrication, the grating period is determined by the intersection angle of the laser beams and light wavelength [22], and thus a higher spatial-frequency can be easily achieved by increasing the intersection angle.

Diffraction efficiency versus applied voltages of the H-PSBPLC grating is plotted in Fig. 3(a). The grating is driven with a 1-kHz square-wave voltage-source and the diffraction efficiency η is obtained as the ratio of the first diffracted order intensity to the total intensity at $V = 0$ [16, 25]. It can be seen that the diffraction efficiency $\eta \approx 0.9\%$ if the voltage is off. The diffraction efficiency decreases to zero at an applied voltage of 50 V, and then increases with the increasing of applied voltage. When the applied voltage is 200 V, the diffraction

efficiency reaches 19.7%. Figs. 3(b) and 3(c) are the diffraction patterns of H-PSBPLC grating probed using a 633 nm He-Ne laser beam at 0 V and 200V, respectively.

At the voltage-off state, the PSBPLC is optically isotropic. The weak diffraction effect comes from the small index mismatch between the PSBPLCs in bright and dark regions. Due to the diffusion of monomers under non-uniform exposure, the average volume fractions of the polymer chains is larger in bright regions than that in dark regions. Since the refractive indices of the polymer chains and the LC mismatch in our experiment, the average refractive indices of the PSBPLCs in bright and dark regions are slightly different, and thus weak diffraction occurs. This diffraction effect is very small and can be completely eliminated if appropriate monomers with matching indices are chosen.

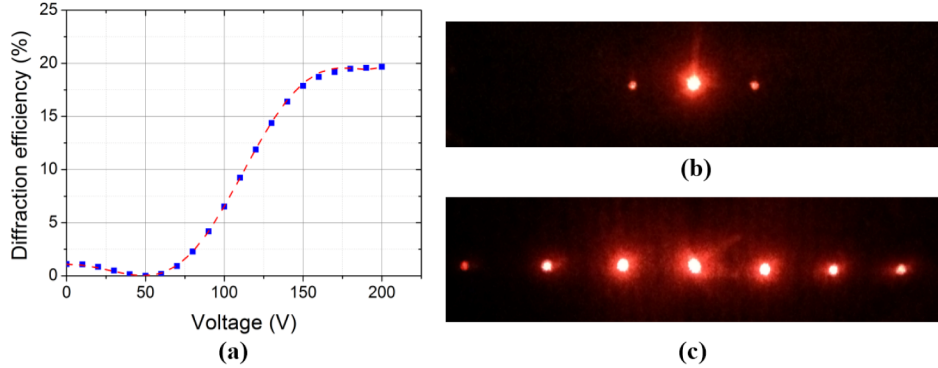


Fig. 3. (a) Measured first-order diffraction efficiency versus applied voltage of the H-PSBPLC grating (blue squares) and simulation results (red dash curve); Diffraction patterns of the H-PSBPLC grating probed using 633nm He-Ne laser beam with a 1 KHz square-wave voltage source at (b) 0 V and (c) 200 V.

When a vertical electric field is applied, periodic electric-field-induced birefringence distribution is obtained due to polymer chain concentration variation. Since the interference light intensity varies sinusoidally, the change of polymer chain concentration is also continuous, and the induced birefringence is non-uniform even over a small region [26]. Here, for simplicity, a theoretical model with two average index values is applied. The refractive index contrast between bright and dark regions under a uniform vertical electric field can be expressed as

$$\delta n_o(E) = n_{o,B}(E) - n_{o,D}(E), \quad (3)$$

where $n_{o,B}(E)$ and $n_{o,D}(E)$ are the induced ordinary indices in bright and dark regions, respectively. Equation (1) can be expanded into Taylor series. As we substitute the series into Eq. (2) and Eq. (3), the index contrast is expressed as

$$\delta n_o(E) = n_{iso,B} - n_{iso,D} - \frac{\lambda}{3} \sum_{i=1}^{+\infty} (K_{B,i} - K_{D,i}) E^{2i} = \Delta n_{iso} - \frac{\lambda}{3} \sum_{i=1}^{+\infty} \Delta K_i E^{2i}, \quad (4)$$

where, λ is the wavelength, $\Delta n_{iso} = n_{iso,B}(E) - n_{iso,D}(E)$ stands for index mismatch between the PSBPLCs in bright and dark regions at voltage-off state, $\Delta K_i = K_{B,i} - K_{D,i}$, represents the different value of i -order coefficient between $\Delta n_B(E)$ and $\Delta n_D(E)$, $K_{B,i}$ and $K_{D,i}$ represent the i -order coefficients of $\Delta n_B(E)$ and $\Delta n_D(E)$, respectively.

The first-order diffraction efficiency can be expressed as [22]

$$\eta = J_1^2 \left(\frac{2\pi d \delta n_o(E)}{\lambda} \right) = J_1^2 \left(\frac{2\pi d \Delta n_{iso}}{\lambda} - \frac{2\pi d}{3} \sum_{i=1}^{+\infty} \Delta K_i E^{2i} \right), \quad (5)$$

where J_1 is the first-order Bessel function of the first kind, and d is the thickness of the grating. According to Eq. (5), a simulation was carried out, where we set $\Delta n_{iso} = -1.058 \times 10^{-3}$, $\Delta K_1 = -8.7 \times 10^{-4} \mu\text{m}/\text{V}^2$, $\Delta K_2 = 6 \times 10^{-6} \mu\text{m}^3/\text{V}^4$, $\Delta K_3 = 2.94 \times 10^{-8} \mu\text{m}^5/\text{V}^6$, and $\Delta K_4 = -3.15 \times 10^{-10} \mu\text{m}^7/\text{V}^8$, and the higher order terms were ignored. The simulation result of the diffraction efficiency is also plotted in Fig. 3(a), and match well with the experimental result.

The diffraction efficiency of the H-PSBPLC grating is mainly determined by the maximum refractive index contrast δn_{max} between bright and dark regions. There are two major factors affecting δn_{max} . The first one is the polymer-concentration gradient between bright and dark regions. Experimental conditions such as exposure time, intensity and temperature, and concentrations of monomers, LC host and photoinitiator have great effects on the monomer diffusion process, resulting in different polymer-concentration gradient [22, 26]. Therefore by optimizing the experimental parameters, a larger δn_{max} and a higher diffraction efficiency could be achieved. The second factor is the intrinsic birefringence of the host LC, which determines the saturation induced birefringence in PSBPLCs [23]. Thus employing large Δn LCs would also contribute to a higher diffraction efficiency.

The operating voltage of the grating is highly dependent on the Kerr constant difference between bright and dark regions, which is ΔK_1 in Eq. (4) [23]. A larger ΔK_1 indicates a lower electric field E for the same $\delta n_o(E)$ [23], and thus a lower operating voltage. There are two ways to increase ΔK_1 and reduce voltage: 1) increase the polymer-concentration gradient by optimizing the abovementioned experimental parameters; and 2) choose LC materials with large dielectric anisotropy ($\Delta\epsilon$) to boost both Kerr constants and ΔK_1 [27].

We further investigated the polarization-dependency of the diffraction efficiency. As Fig. 4 shows, the measured first-order diffraction efficiency as a function of the polarization angle of the incident linearly polarized 633 nm He-Ne laser beam under 0 V, 100 V and 200 V applied voltages at room temperature, respectively. It can be seen that the diffraction efficiency does not change with the polarization angle, verifying that the H-PSBPLC grating is independent of the incident light polarization. Because the host nematic LC has a positive dielectric anisotropy ($\Delta\epsilon$), the LC director tends to align with the electric field [16]. As a result, the optical axis of PSBPLC induced by the vertical electric field is normal to the substrate. Hence, the diffraction is independent of the polarization of normally incident light.

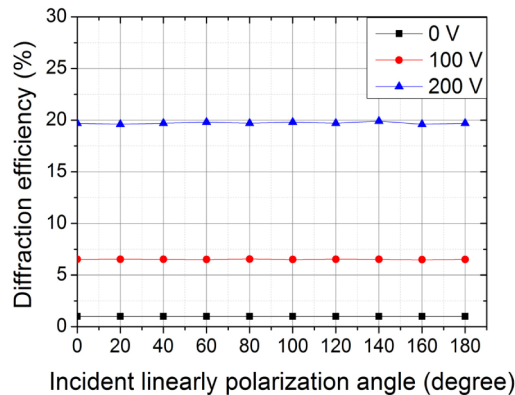


Fig. 4. First-order diffraction efficiency versus polarization angle of incident light under 0 V, 100 V, and 200 V applied voltages, respectively.

The response times were also measured for the H-PSBPLC grating, as shown in Fig. 5. The cell was driven by a 1-kHz 200 V square-wave voltage at room temperature. The rise and decay times are defined as 10% to 90% and 90% to 10% of the diffraction intensity change, respectively. As shown in Fig. 5, the measured rise and decay times for the H-PSBPLC grating are about 300 μs and 400 μs , respectively. Owing to the fast response property of PSBPLC [11], the response times of the grating we fabricated are in the sub-millisecond range.

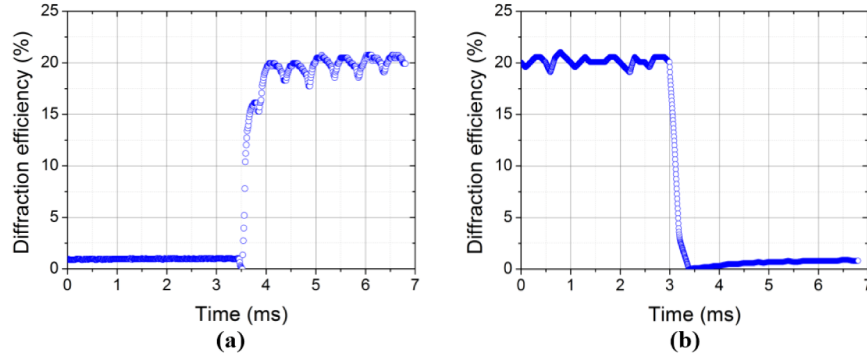


Fig. 5. Electro-optical response of (a) rise time and (b) decay time of the first-order diffraction efficiency of the H-PSBPLC grating.

4. Conclusions

In this paper, we have demonstrated a novel one-step fabrication method for an electrically tunable H-PSBPLC grating. Cured by holographic illumination, the PSBPLC has a periodic polymer concentration distribution. Hence, the induced birefringence varies periodically under a uniform vertical electric field. The diffracted light intensity can be continuously tuned by applied voltage, and the first-order diffraction efficiency reaches 19.7% at 200 V with a cell gap of 20 μm . Good agreement is obtained between simulation and experimental results. The H-PSBPLC grating is polarization-independent, with a small period of $\sim 4 \mu\text{m}$ and a broad temperature range over 70°C . The response times of the grating are in the sub-millisecond range with a 300 μs rise time and a 400 μs decay time. The holographic fabrication method of H-PSBPLC device we proposed is simple and low cost, and thus has great potential for advanced applications such as 3-D displays, light modulators and fast-response optical switches.

Acknowledgments

This work is supported by 973 Program (2013CB328803), National Natural Science Foundation of China (61405114, 61307028), and Science & Technology Commission of Shanghai Municipality (14ZR1422300, 13ZR1420000).